TILTROTOR AEROACOUSTIC CODE (TRAC) PREDICTION ASSESSMENT AND INITIAL COMPARISONS WITH TRAM TEST DATA

Casey L. Burley and Thomas F. Brooks
NASA Langley Research Center
Hampton, VA

Bruce D. Charles
The Boeing Company
Mesa, Arizona

Megan McCluer
NASA Ames Research Center
Moffet Field, Ca

1. ABSTRACT

A prediction sensitivity assessment to inputs and blade modeling is presented for the TiltRotor Aeroacoustic Code (TRAC). For this study, the non-CFD prediction system option in TRAC is used. Here, the comprehensive rotorcraft code, CAMRAD.Mod1, coupled with the high-resolution sectional loads code HIRES, predicts unsteady blade loads to be used in the noise prediction code WOPWOP. The sensitivity of the predicted blade motions, blade airloads, wake geometry, and acoustics is examined with respect to rotor rpm, blade twist and chord, and to blade dynamic modeling. To accomplish this assessment, an interim input-deck for the TRAM test model and an input-deck for a reference test model are utilized in both rigid and elastic modes. Both of these test models are regarded as near scale models of the V-22 proprotor (tiltrotor). With basic TRAC sensitivities established, initial TRAC predictions are compared to results of an extensive test of an isolated model proprotor. The test was that of the TiltRotor Aeroacoustic Model (TRAM) conducted in the Duits-Nederlandse Windtunnel (DNW). Predictions are compared to measured noise for the proprotor operating over an extensive range of conditions. The variation of predictions demonstrates the great care that must be taken in defining the blade motion. However, even with this variability, the predictions using the different blade modeling successfully capture (bracket) the levels and trends of the noise for conditions ranging from descent to ascent.

2.   SYMBOLS

BPF	rotor blade passage frequency (70Hz)
BVI	Blade Vortex Interaction
BVISPL	integrated sound pressure level of the 5th to 40th BPF harmonics, dB
dB_0	constant dB level used to offset measured and predicted dB noise levels
c	reference blade chord, ft
C_N	local blade normal force coefficient
C_{N0}	normalization factor for the local blade normal force coefficient
C_T	rotor thrust coefficient, $T/\rho_0 R^2(\Omega R)^2$
c_0	freestream speed of sound, ft/s
M	Mach number, U/c_0
M_{tip}	rotor hover tip Mach number, $\Omega R/c_0$
p	acoustic pressure, Pa
p_0	constant used to normalize p
r	radial distance along blade from hub, ft
R	rotor radius, ft
T	total rotor thrust, lbf
x	streamwise coordinate from rotor hub (positive downstream), ft
y	crossflow coordinate from rotor hub (positive starboard), ft
z	vertical coordinate from rotor hub (positive up), ft
α_s	rotor shaft angle with respect to x-axis, as measured in wind tunnel, deg
α'	rotor shaft angle, corrected for wind tunnel open jet boundary, deg
Γ	vortex circulation, ft²/s
μ	rotor advance ratio, $V/(\Omega R)$
σ	rotor solidity (thrust weighted)

blade azimuth angle (0^0 aft), deg
rotor rotation frequency, rad/s

3. INTRODUCTION

For the tiltrotor to be successfully integrated into the civilian aviation market, it must be perceived as an acceptably quiet, safe, and economical mode of transportation. The noise impact of these aircraft, particularly during descent and ascent from airports, has been identified as a barrier for civil tiltrotor acceptance. In 1991, a NASA/FAA sponsored report by Bell-Boeing (ref. 1) identified several enabling technologies for the development of a civil tiltrotor aircraft. The Short Haul Civil Tiltrotor (SH(CT)) Program under the Advanced Subsonic Transport (AST) initiative was tasked to address the critical issues that would enable the acceptance of the civil tiltrotor aircraft (ref. 2). Under this program a number of both flight and wind tunnel tests have been conducted to investigate and demonstrate advanced civil tiltrotor technologies. A number of these tests are reported in the literature (refs. 3-13). The flight tests mainly focussed on determining safe, noise abatement procedures and the wind tunnel tests mainly focussed on determining the aerodynamic and acoustic characteristics from different low noise proprotor designs. Tiltrotor aeroacoustic prediction methodologies and analyses are also being developed and validated as specific data become available. These analyses are then implemented into the TiltRotor Aeroacoustic Code TRAC (refs. 14-17).

The TRAC system was initially introduced in reference 15. As explained in that reference, the baseline TRAC system was being developed by integrating existing analyses that were developed and validated in most part for helicopters. A main component chosen for the baseline TRAC system was the comprehensive rotorcraft code CAMRAD.Mod1 (ref. 16). This is a highly modified version of the original Comprehensive Rotor Analytical Model of Rotorcraft Aerodynamics and Dynamics (CAMRAD) (Ref. 18). This code basically consists of three implicitly coupled analyses or unknowns; rotor blade motions, rotor wake, and rotor blade aerodynamics that are required to compute a trimmed rotor state. The recent developments and validation for the wake and blade aerodynamic models reported by Brooks et al (ref. 14), in part was possible because one of the unknowns (blade motions) was eliminated by using measured data (ref. 19). This allowed much progress to be made in not only development but also validation of the unique multi-

core roll-up wake model and the high-resolution airloads analysis, HIRES. These models have been shown to accurately predict helicopter blade aerodynamics and wake characteristics required for accurate BVI noise predictions (refs. 14, 15, 19, 20). Validation of these models for tiltrotor applications has been ongoing, as data becomes available.

Initial TRAC correlations utilizing the baseline TRAC system were reported in 1996 (ref. 15) for a test of an isolated 15% V-22-like proprotor called the JVX. In that test the main objective was to assess the acoustic directivity and BVI noise characteristics for realistic flight conditions. Hence, only acoustic data were obtained and focussed on test parameter variations for flight vehicle glide slope. Fortunately, two rotor angle sweeps, each at a different advance ratio and rotor thrust were obtained. These were utilized for the initial TRAC code validation. Since only acoustic data were obtained for that test, TRAC predictions for blade loads, blade dynamics and wake geometry could not be validated or verified. However the comparison between TRAC acoustic predictions and the JVX measured acoustics was quantitatively quite successful. In addition the predictions also proved to provide insight and plausible explanation for the unique tiltrotor BVI noise trends seen in the measured data.

The TRAC JVX correlation study even though successful, also identified analyses that needed improvements and parts of the TRAC system that required development. The JVX predictions indicated that the tiltrotor, compared to helicopter rotors, tended to be more heavily loaded inboard of the tip region and had a negatively loaded tip for the advancing side, for large ranges of flight conditions. This was predicted to produce a wake consisting of at least two vortex trailers of opposite sign. Since no tiltrotor data was available to verify these findings, alternate means for verification were sought. Experimental wake data from highly twisted blades (refs. 21-23) and CFD simulations (refs. 24-26) of tiltrotors provided some additional insight and support for the JVX prediction results.

In the TRAC development, emphasis has not only been placed on prediction analyses development but integration of the different analysis into a cohesive TRAC system. This involved development of standardized input and output formats for such data as airloads, wakes, blade motions, and acoustics. This standardization enabled the data files to be easily utilized by the different analyses within TRAC and also allowed for efficient implementation of new or replacement codes. The standardized formatting also

forced coordinate system definitions to be identified. This has proven to be invaluable with comparing to test data and as well as predictions from other analysis.

Most recently, as planned under the SH(CT) Program, a tiltrotor aeroacoustic database specifically to validate TRAC was obtained. In 1998, the Tilt Rotor Aeroacoustic Model (TRAM) was tested in the Duits-Nederlandse Windtunnel (DNW). The test was a joint effort of NASA, the U.S. Army and Boeing. The TRAM configuration tested was an isolated 25% of full-scale rotor and nacelle V-22 model. This test represents the first extensive aeroacoustic database for an isolated proprotor (ref. 27). Acoustics, blade airloads and limited wake data (refs. 28-30) were obtained for systematic variations of rotor flight angle, advance ratio, and thrust. One of the major objectives of this test was to provide a database that was of high quality for code validation of TRAC.

The purpose of this paper is twofold. The first is to assess the sensitivity of the baseline TRAC system to inputs, operating condition changes, and blade model choices. And second, it is to correlate TRAC acoustic predictions with recently obtained tiltrotor data from the TRAM test. The main objectives of this TRAC assessment are (1) to determine TRAC prediction sensitivity to blade motion modeling, rotor hover tip Mach number changes, and blade twist and chord changes, (2) to evaluate if such sensitivities are realistic, and (3) to identify analyses that need improvement and corresponding data that are needed to help accomplish such improvement. Employing the input decks (blade and rotor geometric and dynamic descriptions) for two similar tiltrotor models performs examination of the sensitivities. The first is a newly developed (interim) TRAM input deck and the second is an input deck (that is hereby regarded here as a Reference input deck) for the previously reported JVX proprotor test. Details of the predicted aerodynamics, wake, blade motion and acoustics are shown. TRAC acoustic prediction correlations with TRAM data are presented for operating conditions ranging from descent to ascent for different advance ratios and thrust settings. For comparison, trend results using the input deck of the Reference (JVX) rotor run at the TRAM conditions are also presented.

4. PREDICTION METHODOLOGY

The aeroacoustic predictions presented in this paper are made using the TRAC prediction system. TRAC consists of separate CFD (computational fluid
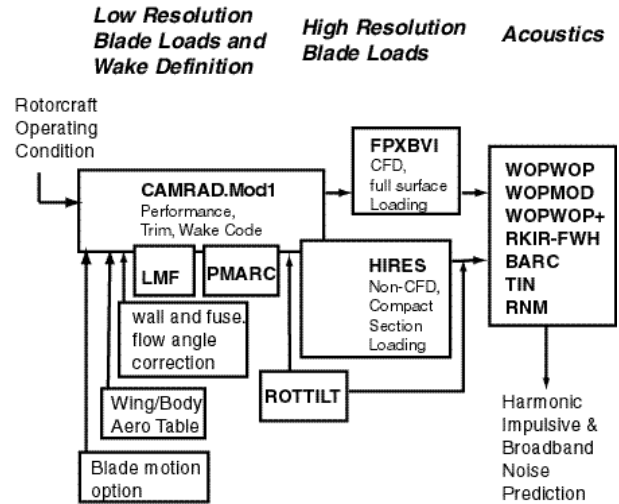

Figure 1. Schematic shows the TiltRotor Aeroacoustic Code, TRAC prediction system.

dynamics) and non-CFD rotorcraft performance, aerodynamic, wake and acoustic analysis programs, along with associated interfaces. A system calculation commences with the rotor trim, wake and performance analysis, which then are used to determine high-resolution blade airloads. These airloads are then used by the rotor acoustic analysis to predict the noise at given observer locations. The TRAC analysis codes are shown schematically in Figure 1. For this validation paper, only results from the baseline codes CAMRAD.Mod1, HIRES and WOPMOD are presented.

The other analysis codes shown are at different stages of development. These capabilities include prediction of tiltrotor fountain flow noise with ROTTILT and TIN (refs. 31, 32), fuselage surface pressures for input to interior noise analysis (ref. 10), high resolution rotor airloads from the CFD code FPXBVI (ref. 33), multiple freewake trailers with LMF (Langley-Maryland Freewake) code is a modified and enhanced version of the Maryland Freewake Code, (ref. 34), rotor body effect on the rotor trim and wake via the CAMRAD.Mod1/PMARC coupling (ref. 35), high-speed impulsive and quadrupole noise (refs. 36-39), broadband self noise and (Blade Wake Interaction) BWI noise (refs. 40, 41) with BARC, noise propagation with RNM (ref. 42) and aeroacoustic optimization procedures using TRAC (ref. 43).

The comprehensive rotorcraft code CAMRAD.Mod1 is used to obtain the rotor trim and performance by predicting the aerodynamics, blade

motion and wake. To provide consistency with the earlier JVX TRAC predictions (ref. 15), the same CAMRAD.Mod1 modeling parameters were also utilized in this work. The modeling parameters include the multi-core roll-up wake model inputs, the number and location of the aerodynamic segments, the blade dynamic model computational inputs, trim options, and the trim, motion and circulation iteration tolerances.

To predict high-resolution airloads, the non-CFD (HIRES) approach is used for this paper. This approach has been shown to be accurate for subsonic to low-transonic conditions for which lifting line, 2-D airfoil analyses are typically valid. The HIRES aerodynamic model is based on the indicial blade response model of Beddoes (refs. 44 and 45). The indicial approach is used since it is valid for arbitrary step size in impulsive loading conditions.

The high-resolution airloads, as well as the blade motion, are utilized in the acoustic analysis WOPMOD to determine the acoustics at a given location. In this paper the predictions are made at each of the microphone measurement locations of the TRAM test. WOPMOD is basically identical to WOPWOP (ref. 46), but modified to directly accept the blade description, blade motion and blade aerodynamics from general file formats that are output from the other TRAC codes. This has greatly simplified and reduced errors associated with coordinate systems, file formats and data handling from the different analyses within the TRAC system.

5. TRAC MODELS FOR THE TRAM AND REFERENCE PROPROTORS

The recently developed input deck for the TRAM rotor and the Reference JVX rotor input deck, previously reported in reference 15, are used in the TRAC sensitivity assessment. The TRAM deck is considered at this time to be an interim deck, since this is the first time any predictions have been made with this and not all TRAM information is completely verified and accurately documented the time of this writing.

TRAM blade motions were computed using the internal modal based analysis of CAMRAD.Mod1. (As previously mentioned, this internal analysis was bypassed in another validation effort by utilizing measured blade motions directly as input to CAMRAD.Mod1 (refs. 14 and 16). The dynamic

modeling of a proprotor, with its high twist and large variation in blade chord and thickness, is a challenge, especially within the context of the lifting line assumptions of CAMRAD.Mod1. In addition, the TRAM rotor blade assembly consists of not only the rotor blade, but also a pitchcase/grip and the yoke, which also serve as dual load paths. The hub load and blade dynamics model within CAMRAD.Mod1 (which corresponds to original CAMRAD for dynamic modeling) is currently limited to a single load path to the hub. CAMRAD.Mod1 only has limited ability to model the root geometry details of a rotor system (refs. 16, 18). For this prediction effort, the rotor was modeled using the cantilever hub option with gimbal and a nominal pitch/gimbal coupling of –15 degrees. The blade dynamics model of CAMRAD.Mod1 requires as input the blade structural properties as well as the rotor control stiffness or frequencies. Since measured values are not yet available, computed values from either the TRAM design and development analyses (NASTRAN) and or design drawing data were used for these inputs. (For the Reference JVX model, Mykelstad - a similar analysis - was used.)

For the TRAM CAMRAD.Mod1 blade dynamics model, the first two blade bending modes and two torsion modes were utilized. This is consistent with that used for the previous JVX validation (ref. 15). The first and second blade bending frequencies and first blade torsion frequency are matched to the values provided by TRAM design analyses and review reports. This matching could only be achieved by decreasing (uniformly) the blade chordwise bending distribution, flapwise bending distribution and torsional stiffness distribution values. Without this matching the frequencies differed from the design analysis values by 10-30%. Without knowing the actual position of the blade as a function of rotor azimuth, it is difficult to determine or assess the CAMRAD.Mod1 blade dynamics model. In order to bracket the effect (and to provide a sanity check) of the predicted elastic blade motions on the results, predictions are presented for both a completely rigid rotor (no elastic blade and control system modes used) and the elastic rotor (2 bending and 2 torsion modes) modeling. The rigid blade comparison is appropriate, as the TRAM blades are known by design to be 'stiff'.

In the course of this work, the sensitivity of the predictions to blade motion detail suggested the need to reference results to an additional proprotor code model. For the JVX test (which was a V-22 Mach number matched test), the prediction comparisons with

measurements proved to be quite successful, reference 15. In that study, the same CAMRAD.Mod1 blade dynamics model, was utilized. However, a number of blade properties were measured and or predicted properties verified with measurement and hence more confidently specified. For this reason, the JVX computational model is used for reference comparisons in this paper.

A comparison of rotor dimensions between the TRAM and the "Reference" JVX rotor are provided in Table 1. The JVX rotor blade chord has more solidity, with the chord and thickness being about 9% larger than the TRAM blade chord and thickness for the same scale rotor. The chord and twist distributions from these two models rotors are compared in Figure 2. The twist distribution of the JVX varies slightly from that of the TRAM from about r/R=0.80 on inboard. The modified twist distribution for the JVX partially compensates for the larger chord, but it is not exact, as the lift distribution deviates somewhat from the V-22 (and TRAM). In order to eliminate any relative effect of the grid distribution for the dynamics definition, the same spanwise distributions for the input properties were used for the TRAM deck as had been previously used for the reference JVX model deck. Aerodynamic properties were defined at 27 spanwise locations and the structural properties defined at 51 spanwise locations.

It is noted that in the prediction comparisons of this paper, the results from the different rotor input-decks are compared on a normalized distance basis. Therefore, proper rotor rpm for the specific size model is used and the scaling of neither the TRAM or the Reference JVX blade structural properties are not necessary.

6. TRAM TEST DESCRIPTION

In the TRAM test, acoustic directivity, blade surface pressures, performance, and blade structural loads data were obtained for a range of advance ratios (including hover), shaft angles, and rotor thrust conditions. Wake measurements were acquired for selected BVI conditions. The TRAM rotor was operated in helicopter and airplane mode configurations.

The isolated TRAM model was designed as a 25% scale model of the starboard V-22 Osprey proprotor. It is a three-bladed, 9.5 ft diameter proprotor with rotor blades that are dynamically scaled to the V-22 rotor. For this test, limits on the drive train vibration levels

prevented running at the full-scale V-22 speed. The nominal constant rotation speed corresponded to a hover tip Mach number of 0.63. This is 88% of the full-scale V-22 hover tip Mach number of 0.71. The rotor is nacelle mounted on a motor housing/sting assembly as shown in Figure 3 for the TRAM rotor in helicopter mode.

Acoustic data were acquired with a thirteen-microphone array, which was located in a plane 1.73R below the rotor hub. (This distance was maintained independent of test condition.) The array was traversed streamwise from –2.76R upstream of the hub to 2.76R

Test Rotor:	TRAM	JVX
V22-scale	25%	15%
Number of blades	3	3
Rotor radius	4.75 ft.	2.85 ft.
Tip chord	5.5 in.	3.6 in.
Rotor solidity,	0.105	0.114
Precone angle	2 deg.	2 deg.

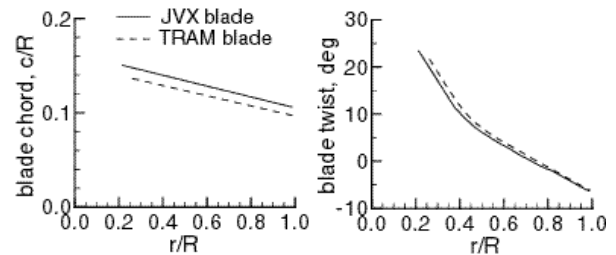Table 1. TRAM and JVX (Reference) rotor descriptions.

Figure 2. TRAM and JVX blade chord and twist distributions.

Figure 3. Isolated Rotor TRAM installed in the DNW test section with the microphone wing array located under the rotor.

downstream of the hub. The traverse was stopped to acquire data at each chosen measurement (grid) location.It is noted that the motor housing sting was treated with acoustic foam, and was found to successfully minimize reflections. However, a number of the microphone locations on the retreating side of the model were shielded. The retreating side acoustic measurements may not be realistic and are not a focus of this study, although included.

The details of noise data acquisition and processing procedure is reported in reference 28. The same data processing procedures were also used to acquire acoustic data for the JVX test. For the data presented both here in this report and references 3 and 15, the measured noise spectra are integrated on a power basis using all frequency bands from the 5th to the 40th rotor harmonics, to serve as a metric to represent the BVI components of the total noise. These integrated levels, referred to here as BVISPL, are used to produce BVI directivity contour plots for given rotor operating conditions. All measured and predicted acoustic results presented in this paper are normalized or offset by a constant, that is, the BVISPL metric values are offset by a constant dB_0 value, and the acoustic pressure is normalized by constant p_0.

7. TRAC PREDICTION SENSITIVITY

In this section the TRAC prediction sensitivity to rotor speed, blade twist, chord and blade motion modeling is examined. Since the comparative rotors are not the same size, the blade motion, aerodynamics, and acoustic predictions are performed at locations based on the respective rotor radius. For example, for both the TRAM and Reference (JVX) rotor, acoustic predictions are made for observer locations on a plane that is located $z/R=1.75$ below the rotor hub. Also, by using normalized lengths, the scaling of either the TRAM or the Reference blade structural properties is not necessary, as previously discussed. For all predictions, both rotors (the TRAM and Reference rotor) are trimmed to the measured TRAM test thrust and measured TRAM hub flap angle values. Trim was accomplished by varying the collective and cyclic pitch controls, which was the trim procedure used in reference 15. The measured TRAM test lateral and longitudinal flap angles for most of the acoustic test cases are on the order of 0.2 to 0.6 degrees. (Note, however, in the actual JVX test, (ref. 3) the measured flap angles were essentially zero.)

Wind tunnel wall corrections to the mean rotor angle of attack (measured shaft angle) were used in the predictions. The wind tunnel wall corrections were determined by the Langley developed code (refs. 47, 48). The angle corrections are dependent on the tunnel configuration, rotor size and location within the test section as well as C_T, rotor rpm and μ. For the TRAM rotor and the Reference rotor in the open test section of the DNW, the corrections range between $-0.8°$ to $-1.6°$.

## Sensitivity of blade wake geometry to proprotor speed

Since the TRAM was operated at 88% of JVX test rotor speed (which is also 88% of the V-22 rotor speed), and the JVX input deck is the Reference rotor deck for this present study, the effect of this speed reduction on the predicted results is examined. Calculations are performed for both the elastic blade model and a corresponding rigid blade model, for a particular flight condition where BVI noise is important, and where a JVX test condition matched that of a TRAM test condition. The blade tip flap and pitch motion are shown in Figure 4 for the Reference rotor, predicted at the full rotor speed ($M_{tip}=.71$) and at 88% speed ($M_{tip}=.63$). The flap angles shown include that due to first harmonic flapping as well as the elastic blade assembly bending. The 2° precone is not included. The pitch angles shown include that due to cyclic stick control and blade assembly torsional deflection. The collective pitch and pitch/gimbal coupling angle are not included. For the rigid blade cases, the flap angles are essentially identical and the pitch angles are nearly so. The motions of the elastic blades are seen to experience a droop, due to rotation, of less than 1° from the preconed tip position. The trimmed pitch angle variations at the tip are seen to be less than the rigid blade amplitudes. At the higher speed ($M_{tip}=.71$) the elastic blade results have high frequency fluctuations about the one-per-revolution pitch and flap cyclics. These fluctuations, particularly for the pitch, do not exist when the Reference JVX rotor is trimmed to zero flapping. (previous JVX predictions of reference 15, used the measured JVX test flap angles of essentially zero.) The fluctuations appeared when the (non-zero) measured TRAM flap angles were input to TRAC. For the condition in Figure 4, the measured TRAM lateral and longitudinal flap angles are about 0.4°.

The predicted vortex wake geometry (frozen in time at one instant, and viewed from above the rotor

disk) is shown in Figure 5, for the blade conditions corresponding to Figure 4. One blade position is shown (ψ=160^0) for reference. The wake calculations use the vortex multicore roll-up modeling (ref. 14) in CAMRAD.Mod1. The vortex modeling depends on the spanwise blade loading distributions and a special rotor algorithm, which is an extension of the Betz (ref. 49) roll-up modeling approach for fixed wings. The present algorithm in CAMRAD.Mod1 is limited to two trailed-vortex elements — a tip vortex (shown as solid lines in Figure 5) and a secondary vortex (shown as dashed lines). The secondary vortex tends to occur when the tip is negatively (or lightly) loaded and inboard loading is relatively high. Depending on loading near the tip, the tip vortex can shift inboard at different blade azimuths. This produces the irregular multiple vortex patterns shown in Figure 5. These vortex geometries, along

with the azimuthal variation in vortex strength, produce the unique characteristics found for proprotor BVI noise. The extent to which the vortex wakes reflect reality is the extent to which noise is correctly predicted.

Figure 5 can be used to demonstrate some basic points on scaling and model sensitivity for noise prediction. Consider first the rigid blade. At both Mach number conditions with blade motions being almost matched, the wake is found to have the same general appearance. Because the wake has a critical dependence on the local blade loading, any speed related differences in loading (due to say differences in blade section aerodynamic lookup tables in the code) does not appear to significantly affect trim and loading details. However, the elastic blade rotor produced somewhat different blade motions for the two rotor speeds, and the wake was substantially changed (compare Figure 5a and 5b). The important point here is that small blade dynamic motion differences, even when mean aerodynamic trim conditions are matched,
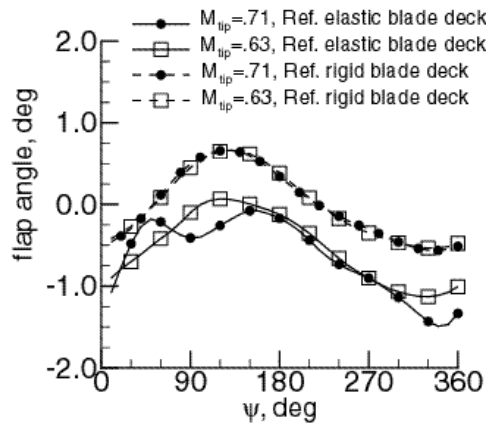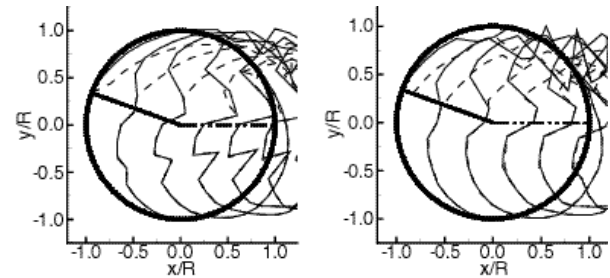

a) Predicted Reference rotor flap angle at blade tip.
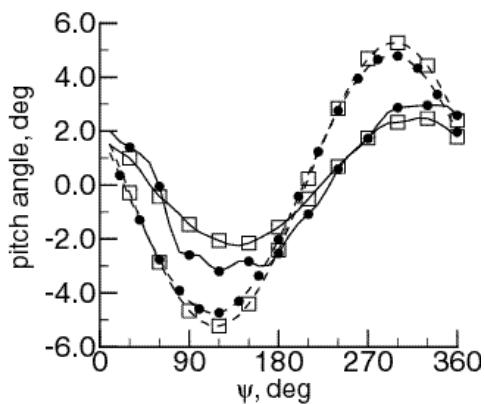
b) Predicted Reference rotor pitch angle at blade tip.

Figure 4. Predicted blade tip flap and pitch angles determined using the rigid and elastic blade motion modeling in the Reference (JVX) model deck. Results are shown for different tip Mach number conditions. (TRAM rotor condition of low C_T, α_s=6°, μ=0.175)
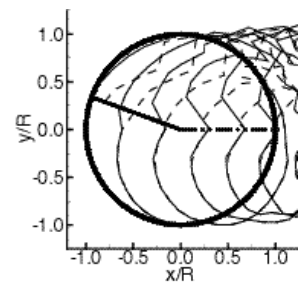

a) Ref. elastic blade deck, M=.71

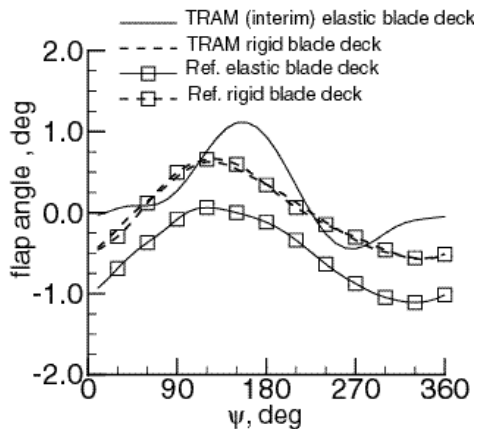b) Ref. rigid blade deck, M=.71
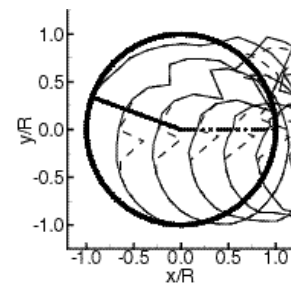
c) Ref. elastic blade deck, M=.63

d) Ref rigid blade deck, M=.63

Figure 5. Top view of predicted wake geometries determined using the rigid and elastic blade motion modeling in the Reference model deck. Results are shown for different tip Mach number conditions. (TRAM rotor condition of low C_T, α_s=6°, μ=0.175).
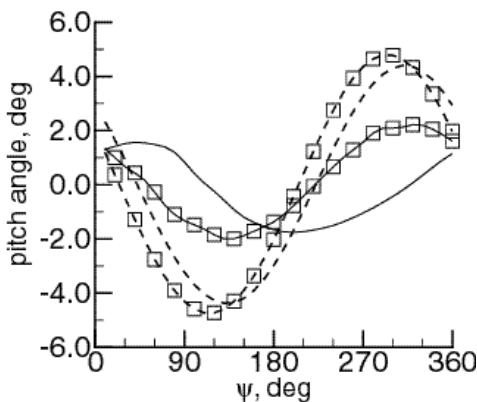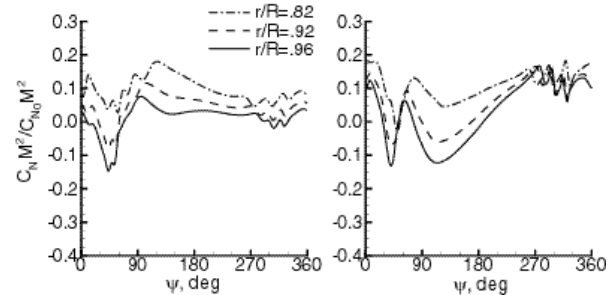
are crucial to wake formation and noise. Subsequently, it is shown that even rigid blades can produce different wakes and noise when blade design differs somewhat (for example, TRAM versus the Reference JVX blade (geometric) shape details).

Blade modeling effect for a TRAM condition

Predicted blade flap and pitch angles determined from the elastic blade decks for both the TRAM and the Reference rotor are shown in Figure 6 for M_{tip}=0.63. The Reference blade deck results were repeated from Figure 4. It is seen that for both rigid blade decks, the flap angle results are essentially identical. The corresponding pitch angles are nearly the same in amplitude and distribution, but offset in phase. This is due to the Reference blade chord and twist being

slightly different than the TRAM (Figure 2). For the elastic blade decks, the trimmed blade motions show distinct differences, with the TRAM blade model having larger tip flap angles and a shift in phase for the pitch angle. The resultant normalized sectional loads, $C_N M^2 / C_{N0} M^2$, for the four cases are shown in Figure 7. The TRAM elastic blade deck (Figure 7a) shows positive loading near the blade tip in the second rotor quadrant ($= 90°$ to $180°$), which is where the flap and blade angles from this deck are larger than the other deck results (Figure 6). The results from the corresponding TRAM rigid blade deck (Figure 7b) shows negative loading in this quadrant due to the lower flap and pitch angles. .The same general relationship is true between the Reference (JVX) elastic and rigid blade model decks. Negative loading in the second quadrant can lead to the release of negative tip vortices and the presence of positive secondary vortices in the roll-up modeling of CAMRAD.Mod1. This is seen in the wake presentations of Figures 5(c) and (d) for the Reference (JVX) blade model and Figures 8(a) and (b) for the TRAM blade model.

a) Predicted TRAM rotor flap angle at blade tip.
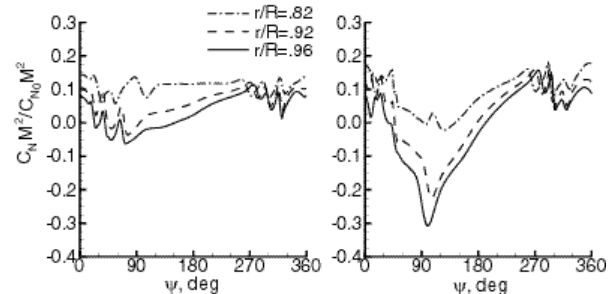

b) Predicted Tram rotor pitch angle at blade tip.

Figure 6. Predicted blade tip flap and pitch angles shown for rigid and elastic blade modeling for the TRAM and Reference rotor model decks. (TRAM rotor condition of low C_T, $_s$=6°, μ=0.175).

a) TRAM (interim) elastic   b) TRAM rigid blade
   blade deck   deck

c) Ref. elastic blade deck   d) Ref. rigid rotor deck

Figure 7. Predicted local blade normal force (normalized) determined using the rigid and elastic blade motion modeling in the TRAM Reference model decks (TRAM rotor condition of low C_T, $_s$=6[0], μ=0.175).

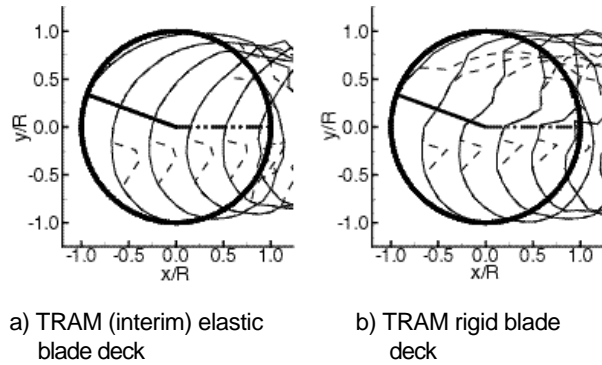a) TRAM (interim) elastic   b) TRAM rigid blade
   blade deck   deck

Figure 8. Top view of predicted wake geometry for the TRAM rotor. (Rotor condition of low C_T, $_s$=6°, μ=0.175).

It was beyond the scope of this study to compare predicted and measured blade loads and wakes. It is noted, however, that references 29 and 30 for the TRAM test show measured negative loading characteristics similar to the rigid model results presented here for a range of rotor conditions. Also, the test showed measured wakes with multiple vortices (measured using a Laser Light Sheet (LLS) technique on the advancing side). Again, this observation agrees with the predicted multiple vortex patterns that were obtained for the rigid model results. Nevertheless, the TRAM flow visualization measurements typically showed 2 or 3 vortices per blade wake trailed, rather, than the 1 or 2 in the predictions. The present algorithm and wake model (ref. 14) limits the predicted number of trailed vortices to two.

Sensitivity of acoustics to blade modeling

Figure 9 shows the top view of the TRAM acoustic measurement grid formed by traversing the microphone wing array to a series of streamwise positions 1.73R below the rotor disk. The TRAM rotor radius R normalizes the streamwise coordinate x and the cross- stream coordinate y. In Figure 10, for the TRAM test case presented, the BVI noise level metric, BVISPL (dB-dB$_0$) is contour plotted based on measurements at the grid points. Two intense noise regions are seen; one related to the advancing side (0<y/R) BVI noise, and the other on the retreating side (y/R<0). The retreating side noise was subject to interference as previously indicated. Also shown, in Figure 10, is a measured average acoustic time history corresponding to location A which is indicated on the TRAM measurement grid in Figure 9. (Note, the acoustic pressure is non-dimensionalized by p$_0$.) Location A is where the Max-BVISPL is measured for the advancing side. Here, the BVI noise pulses in the
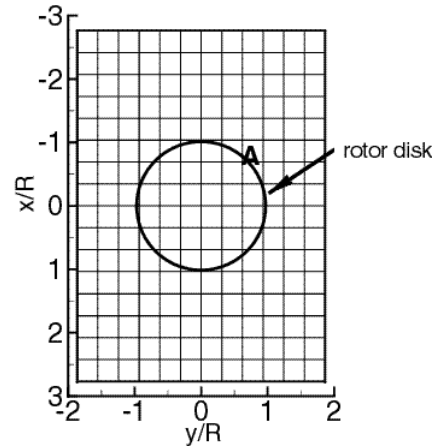

Figure 9. Top view of the TRAM test acoustic measurement grid. Each intersection point is an acoustic measurement location.
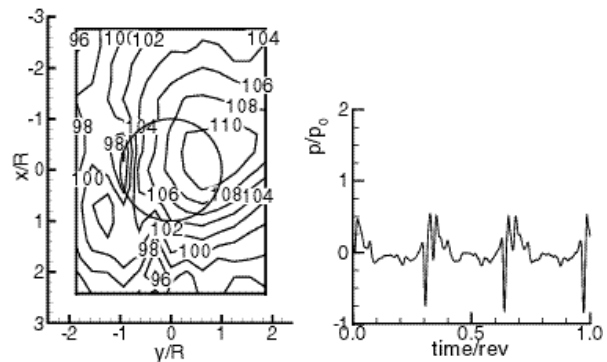

Figure 10. Measured TRAM BVISPL (dB-dB$_0$) contour and measured time history obtained from location-A under the advancing side (Figure 9). (TRAM rotor condition of low C_T, $_s$=6°, μ=0.175).

time history indicate multiple BVI encounters over limited azimuth ranges for each of the three blades.

Figures 11 and 12 present the predicted BVISPL contours and predicted acoustic pressure time histories at location A, which correspond to the measured results in Figure 10. The corresponding predicted blade motions, sectional loading, and wake geometries are given in Figures 6, 7, 8(and 5(c) and (d)), respectively. It is seen that for this test condition, the TRAM rigid blade deck most accurately predicts the noise level contours. The contour predictions performed with the Reference rigid blade deck also have nearly suitable shape and levels as that measured. The time histories at location A offer a somewhat different story. Here the time history overall shape is most accurately predicted
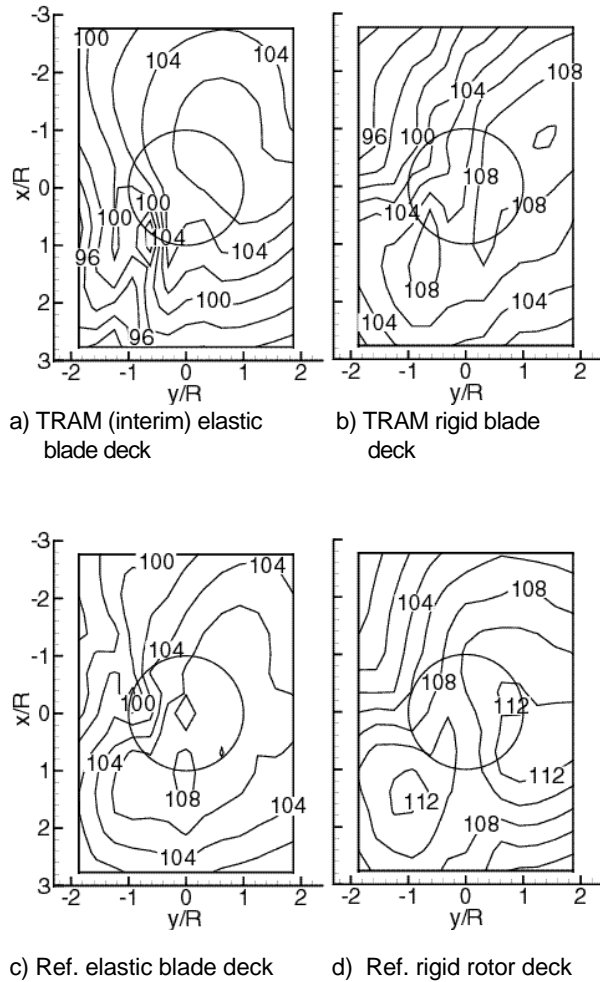
a) TRAM (interim) elastic
   blade deck

b) TRAM rigid blade
   deck

c) Ref. elastic blade deck   d) Ref. rigid rotor deck

Figure 11. Predicted BVISPL (dB-dB$_0$) noise contours for the TRAM rotor at test condition of low C$_T$, $_s$=6°, μ =0.175.

a) TRAM (interim) elastic
   blade deck

b) TRAM rigid blade
   deck

c) Ref. elastic blade deck   d) Ref. rigid rotor deck

Figure 12. Predicted (normalized by p$_0$) acoustic time histories at location A (Figure 9), determined using the rigid and elastic blade motion decks for the TRAM and Reference rotor. (TRAM rotor condition of low C$_T$, $_s$=6°, μ =0.175, M$_{tip}$=.625).

by the TRAM elastic blade deck, although the number of observable BVI events is best seen for the Reference rigid blade deck.

Note that because of phasing differences, caused by time delays between observed BVI-events for any one observer (specific microphone measurement location), one can expect substantial time history differences at different grid locations. Therefore, Figure 12 alone cannot determine to what extent a model captures physical events. Still, certain features can be tied to the wake geometries to add insight to the prediction results. First, the predicted advancing-side wake geometry (Figure 8(a)) shows only a single vortex per blade for the elastic TRAM blade. This appears to correspond to the single pulse events in Figure 12(a), rather than the multiple events seen in the
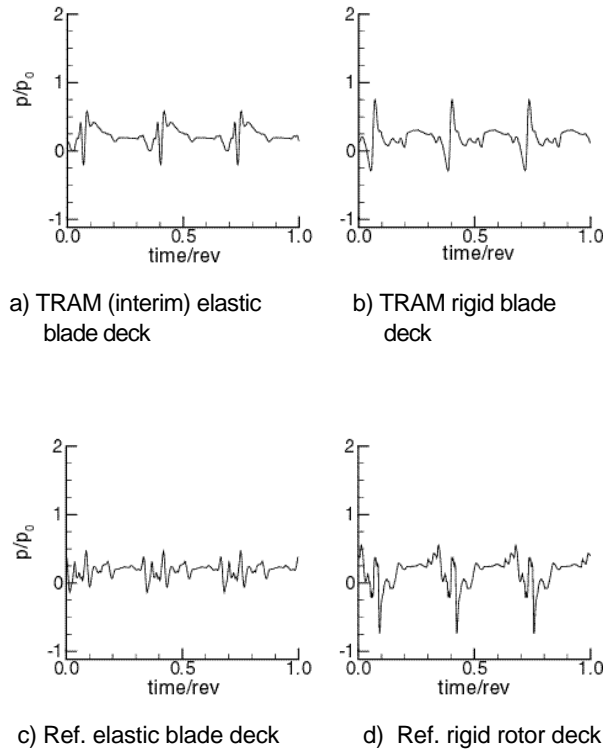
TRAM flow visualization measurements. (Note, however, that multiple events in a blade's rotation are quite possible with only a single shed tip vortex per blade.) But other aspects of the predicted time history are good (peak-to-peak amplitude), suggesting that many important features of the actual blade motion may be captured —but not perhaps the tip motion, which affects the number of vortices.

For the TRAM rigid blade model, multiple shed vortex BVIs are not apparent in the time history. This is consistent with the geometry of the shed secondary vortex (see Figure 8(b)) that is skewed with respect to any advancing side BVI events, rather than being parallel as required for strong BVI noise. The somewhat spiked time histories produced by the Reference blade decks (Figures 12(c) and (d)), correlate to some unrealistic vortex wake geometry features. The jagged tip-vortex dominated wake on the advancing side for the elastic blade case of Figure 5c, results from the wake being released not at the tip but further inboard. The local blade loading at the time of the

vortex emission (ref. 14) determines this spanwise location. Currently, due to lack of data, the wake modeling in CAMRAD.Mod1 does not account for the vortex formation upon release, but assumes a developed (fully rolled-up) vortex upon release. This and the wake discretization creates a jagged appearance in the final wake geometry. These jagged wake edges can protrude upward; resulting in locally spiked BVI occurrences. In reality, this peculiar wake portion may indeed be present in the flow, but likely without jagged geometry details. For the Reference rigid blade model, the tip and secondary vortex wake-geometry details appear more realistic (see Figure 5(d)). The tip vortex, through mutual influence with the secondary vortex is rotated upward which affects the resulting BVI occurrences. With negative circulation tip vortices, the secondary is also elevated somewhat. (These vertical motions cannot be seen in the top view presentation of Figure 5(d).) To the extent this geometry affects BVI noise is seen in Figure 12(d). Many of the characteristics observed above, for the different rotor code models change with different TRAM test operating conditions.

8. TRAC AND TRAM COMPARISONS FOR SHAFT ANGLE VARIATIONS

The maximum levels of the BVISPL noise metric (Max-BVISPL) that are found on the advancing side (second quadrant, where $90° < 180°$) are plotted as a function of proprotor shaft angle in Figures 13 to 17. Each figure represents a shaft angle sweep at a different advance ratio and rotor thrust setting. The experimental results are shown as the solid symbols and the lines with and without symbol are determined from TRAC predictions.

Dual horizontal axes are shown in Figures 13-17. One is the test shaft-angle $_s$ axis and the other is the $´-$ $_{induced}$ scale. Here, $´$ is the shaft angle corrected for the open jet wind tunnel boundary and $_{induced}$ is the mean induced rotor flow angle due to thrust, with respect to the oncoming flow. This is defined by momentum theory (refs. 50 and 51) as $_{induced} = 90C_T/ \mu^2$ (valid for $\mu>0.1$) in units of degrees. It was found that for helicopter rotors, the Max-BVISPL peaks for angles somewhat less than $´-$ $_{induced}$. From Brooks, et al. (refs. 52, 53), for an untwisted blade on a freely-articulated hub, the angle of the peak was less by 2.0°, and for a model BO-105 (hingeless rotor), it was less by 0.5°. These values are designated in Figures 13-17 as helicopter 1 and 2 respectively, along with the apparent TRAM data peak levels, designated as local

peak. This shows that the proprotor obtains peak levels at lower rotor angles than helicopter rotors by an average of about 5°. This is consistent with the idea that multiple vortex shedding occurs over broad $_s$ ranges, due to weak (or negative) loading at the proprotor tip and strong positive loading inboard of the tip. Strong inboard (secondary) vortices induce (push) the tip vortices vertically higher in the wake flow. This allows strong BVI to occur at lower $_s$ than is found for helicopters, where the tip region is more positively loaded. As $_s$ is increased further (steeper descent), the inboard vortices (perhaps multiples) then incur their own strong BVI. These peak interactions at differing $_s$ serve to spread the peak noise region over a lager range of shaft angles than is seen for helicopters.

The Max-BVISPL predictions from the four decks clearly bracket the measured data results and demonstrate the measured data trends. The specific TRAM test condition that was examined in detail in this paper, up to this section, is the $_s = 6°$ case of Figure 15, for low C_T and $\mu = .175$. For all the other test conditions, the relative agreement with the data and relative levels predicted for the different blade models in the codes depended greatly on condition. The differing results from the rigid blade decks are ultimately traced to the aerodynamic differences of the JVX and TRAM blade shapes. The differing elastic characteristics provide additional, and likely the most important, effect on the wake and thus noise. It is found in analyzing
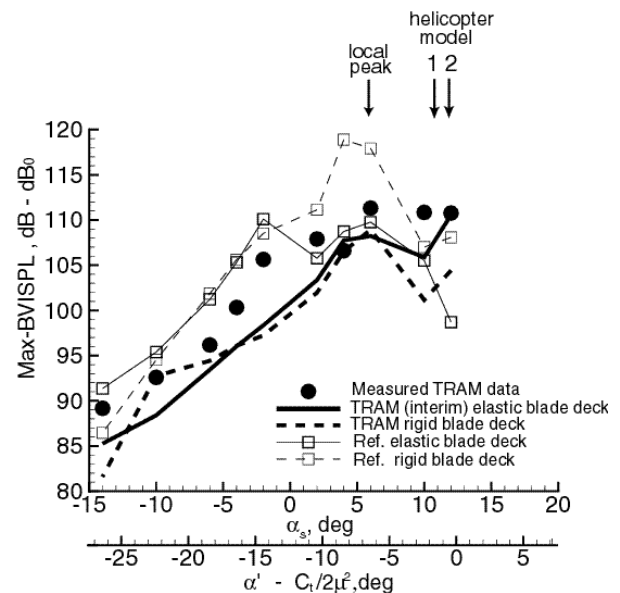

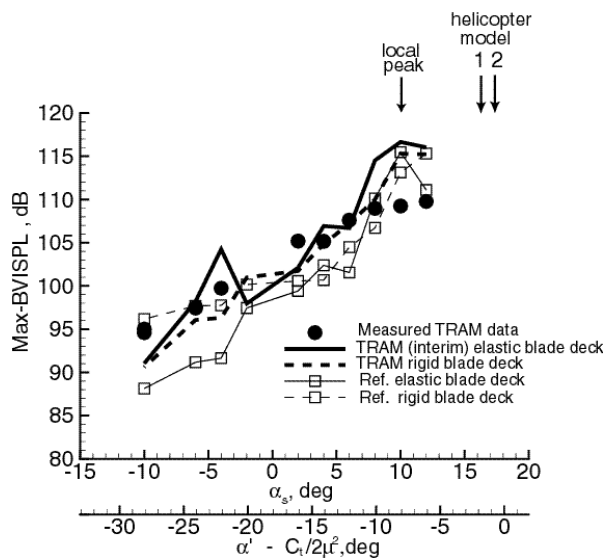Figure 13. Max-BVISPL on advancing side for low C_T condition, μ=0.15.

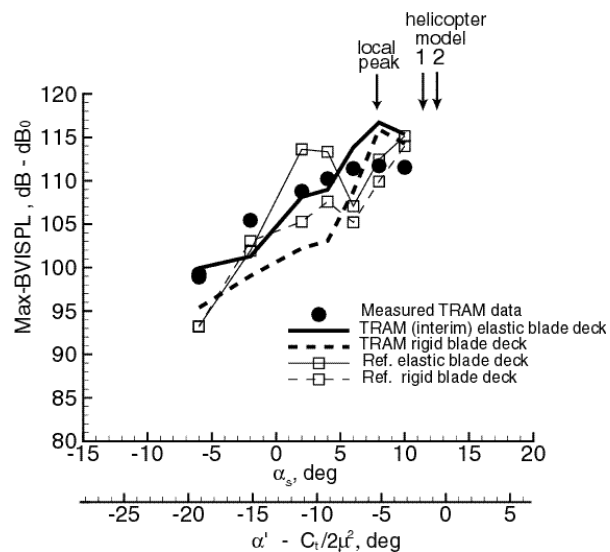Figure 14. Max-BVISPL on advancing side for high C_T condition, μ=0.15.

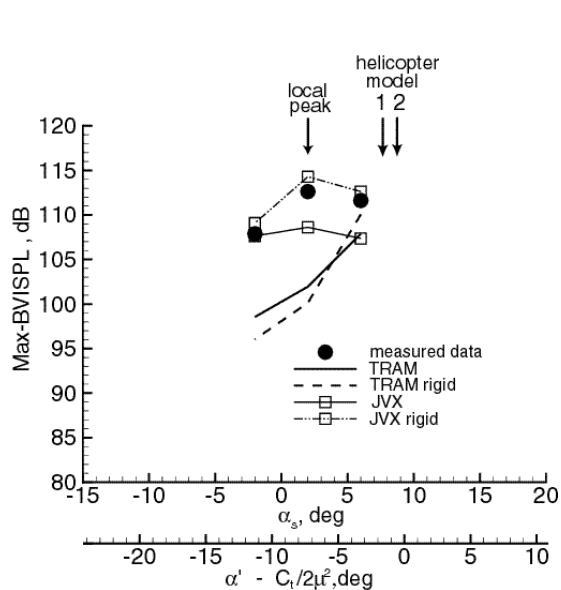Figure 16. Max-BVISPL on advancing side for high C_T condition, μ=0.175.

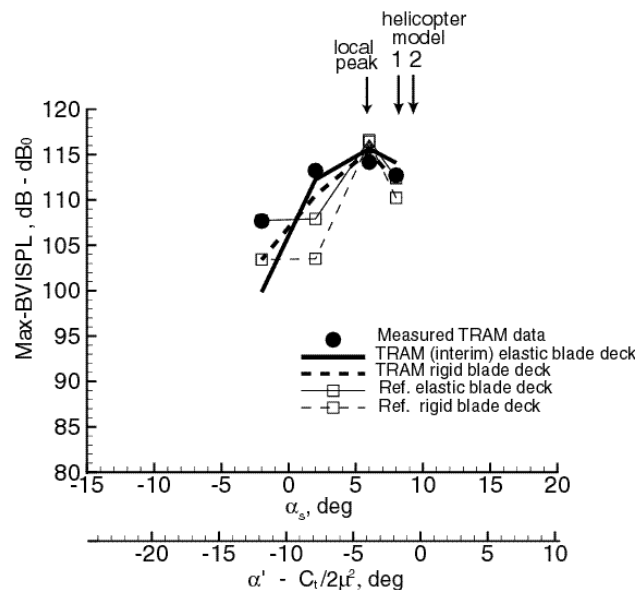Figure 15. Max-BVISPL on advancing side for low C_T condition, μ=0.175.

Figure 17. Max-BVISPL on advancing side for high C_T condition, μ=0.20.

B3 -12

the predictions that the noise levels are generally higher when multiple vortices are produced, but not always. Azimuth dependent tip loading is also a major factor. This variation often causes undulations of the vortex geometry, for single or multiple trailed vortices, potentially increasing opportunities for strong BVI occurrences.

Measured and predicted noise directivities were compared for all the cases shown in Figures 13-17. A limited number of these comparisons are presented in Figures 18-21. Directivities are shown for three shaft angles for the advance ratio $\mu = 0.15$ and at both the low and high C_T conditions. The angles represent conditions of deep-descent ($\alpha_s = 12°$), descent ($\alpha_s = 6°$), and ascent ($\alpha_s = -6°$). Note that for both the deep-descent and ascent conditions, the agreements in directivity shape, as well as level, are generally good. The reduced levels for the ascent (climb) case, $\alpha_s = -6°$, indicates that strong BVI are not occurring. For this condition, the predicted wake is below and away from the rotor disk. For the two descent conditions, $\alpha_s = 6°$ and $12°$, the predicted wakes are near or in the plane of the rotor disk, which result in the high BVI noise levels. The directivities at $\alpha_s = 6°$ are not well predicted. An examination of the trends with shaft
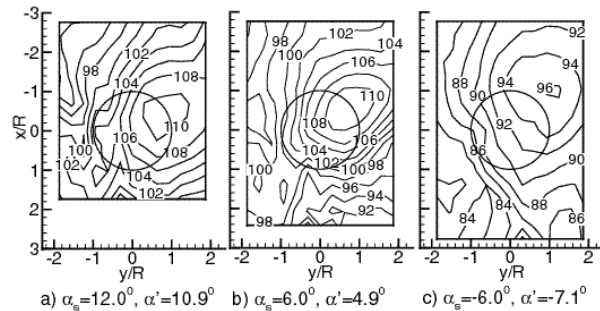

a) $\alpha_s=12.0°$, $\alpha'=10.9°$ b) $\alpha_s=6.0°$, $\alpha'=4.9°$ c) $\alpha_s=-6.0°$, $\alpha'=-7.1°$

Figure 18. Measured BVISPL noise contours for 3 shaft angles for low C_T, $\mu=0.15$.

a) $\alpha_s=12.0°$, $\alpha'=10.9°$ b) $\alpha_s=6.0°$, $\alpha'=4.9°$ c) $\alpha_s=-6.0°$, $\alpha'=-7.1°$
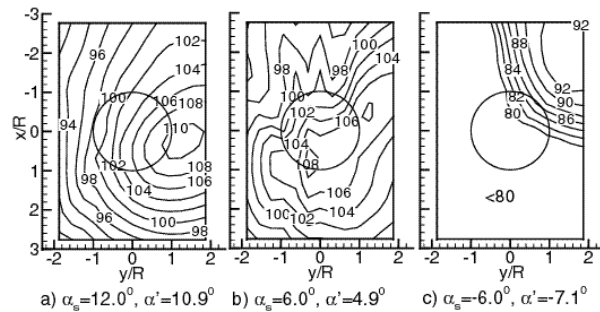
Figure 19. Predicted BVISPL noise contours for 3 shaft angles for low C_T, $\mu=0.15$.

a) $\alpha_s=12.0°$, $\alpha'=10.5°$ b) $\alpha_s=6.0°$, $\alpha'=4.4°$ c) $\alpha_s=-6.0°$, $\alpha'=-7.6°$
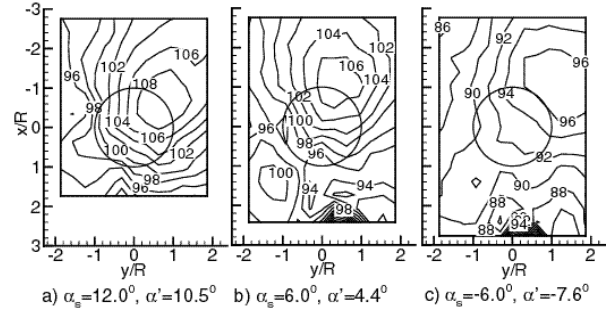
Figure 20. Measured BVISPL noise contours for 3 shaft angles for high C_T, $\mu=0.15$.

a) $\alpha_s=12.0°$, $\alpha'=10.5°$ b) $\alpha_s=6.0°$, $\alpha'=4.4°$ c) $\alpha_s=-6.0°$, $\alpha'=-7.6°$
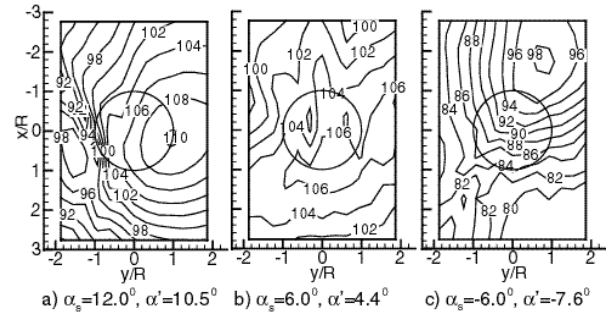
Figure 21. Predicted BVISPL noise contours for 3 shaft angles for high C_T, $\mu=0.15$.

angle (Figures 13 and 14) indicates that at about $\alpha_s = 6°$, the Max-BVISPL starts to level off and decrease with increase in shaft angle. For this to occur, the blade and wake interactions must change and/or the strength of the interacting vortices must be reduced. The predictions are not capturing the details of these changes, which is not unexpected, due to the sensitivity of the predicted wake and blade motion shown in this study.

9. CONCLUDING REMARKS

TRAC predictions are presented for TRAM test conditions obtained for the helicopter configuration. These include large shaft angle sweeps, at both high and low thrust settings, and three advance ratios. The TRAC prediction comparisons serve to assess and validate the baseline prediction codes of TRAC (namely CAMRAD.Mod1, HIRES and WOPMOD) for a proprotor. Because blade motion was not measured (therefore could not be used for validation or as input to TRAC), the validation effort focussed substantially on blade and blade root description modeling that defines the elastic motions. It was found that elastic motion differences, as well as blade geometric details, affect

both the rotor wake and blade loads, and thus the noise, substantially. These differences occur in what aerodynamicists might normally consider equivalent flight trimmed conditions. Still, the TRAC predictions, using the rigid and elastic rotor blade models, clearly and successfully bracket the measured acoustic data and demonstrate the proper acoustic data trends. It also demonstrates the ability to predict and explain the unique tiltrotor BVI noise versus rotor angle dependence.

Much focus in recent years has been on rotor wake prediction. This study demonstrates the need to determine accurate rotor blade motion as well. Blade motions are not only important in determining blade vortex miss distance, but more importantly in properly predicting the details of both the blade loading and wake. This is of particular concern for the proprotor where, in contrast to the helicopter rotor, the blade loading is concentrated inboard and not so much in the tip region. The TRAC vortex roll-up modeling is held to a delicate balance between creating one or two trailed vortices. Blade motion details make the difference. More examination is needed to determine the TRAM blade motions and TRAC sensitivity to these motions. Much of the immerging surface pressure and wake data from the TRAM test will be valuable for this purpose. As for continued TRAC development, in order to attain the robustness and reliability needed, refinements in the wake roll-up algorithms and other wake modeling are needed. This must include the provisions for releasing more than two vortices per blade, free wake refinement, and vortex evolution modeling.

10. ACKNOWLEDGMENTS

11. REFERENCES

1. Berry, D. (Editor), "Civil Tiltrotor Missions and Applications Phase II: The Commercial Passenger Market – Summary Final Report," NASA CR 177576, February 1991.

2. Marcolini, M. A., Burley, C. L., Conner, D. A., Acree, C. W., Jr., "Overview of Noise Reduction Technology of the NASA Short Haul (Civil Tiltrotor) Program" SAE paper 962273, International Powered Lift Conference, Jupiter, FL, November 8-10, 1996.

3. Marcolini, M. A., Conner, D. A., Brieger, J.T., Becker, L.E., and Smith, C.D., "Noise Characteristics of a Model Tiltrotor," 51st AHS Annual Forum, Fort Worth, TX, May, 1995.

4. Conner, D. A., and Wellman, J. B., "Hover Acoustic Characteristics of the XV-15 with Advanced Technology Blades, " AIAA Journal of Aircraft, Vol.31, No. 4, 1994.

5. Edwards, B. D., "XV-15 Low-Noise Terminal Area Operations Testing," NASA CR-1998-206946, February 1998.

6. Lyle, K.H., "XV-15 Structural-Acoustic Data," NASA-TM-112855, June 1997.

7. Polak, D. R., George, A. R., "Flowfield and Acoustic Measurements From a Model Tiltrotor in Hover," AIAA Journal of Aircraft, vol. 35, No. 6, December 1998.

8. Young, L. A., "Tilt Rotor Aeroacoustic Model (TRAM) – A New Rotorcraft Research Facility," Heli Japan 98; Proceedings of the AHS International Meeting on Advanced Rotorcraft Technology and Disaster Relief, Gifu, Japan, April 1998.

9. Liu, S. R., Brieger, J. Peryea, M., "Model Tiltrotor Flow Field/Turbulence Ingestion Noise Experiment and Prediction," 54th AHS Annual Forum, Washington, D.C, May 1998.

10. Lyle, K. H., Burley, C. L., Prichard, D. S., "A Comparison of Measured and Predicted XV-15 Tiltrotor Surface Acoustic Pressures," AHS Technical Specialists' Meeting for Rotorcraft Acoustics and Aerodynamics, Williamsburg, VA, October 1997.

11. Wang, J. M., Torok, M. S. Nixon, M. W., "Experimental and Theoretical Study of Variable Diameter Tilt Rotor Dynamics," AHS Vertical Lift Aircraft Design Conference, San Francisco, CA, January 1995.

12. Conner, D. A., Marcolini, M. A., Edwards, B. D., Brieger, J. T., "XV-15 Tiltrotor Low Noise Terminal Area Operations," 53rd AHS Annual Forum, Virginia Beach, VA, April-May 1997.

13. Edwards, B. D., "XV-15 Tiltrotor Aircraft Noise Characteristics," 46th AHS Annual Forum, Fort Worth, TX, May 9-11, 1990.

14. Brooks, T. F., Boyd, D. D., Burley, C. L., Jolly, R. J., "Aeroacoustic Codes for Rotor Harmonic and BVI Noise-CAMRAD.Mod1/HIRES," AIAA Paper No. 96-1735, 1996.

15. Burley, C. L., Marcolini, M. A., Brooks, T. F., "Tiltrotor Aeroacoustic Code (TRAC) Predictions and Comparison with Measurements," 52nd AHS Annual Forum, Washington, D.C., June 1996.

16. Boyd, Jr., D. D., Brooks, T. F., Burley, C. L., and Jolly, Jr., J. R.: Aeroacoustic Codes for Rotor Harmonic and BVI Noise-CAMRAD.Mod1/HIRES: Methodology and User's Manual, NASA TM 110297, March 1998.

17. Prichard, D. S., Boyd, D. D., and Burley C. L., "NASA/Langley's CFD-Based BVI Rotor Noise Prediction System: (ROTONET/FPRBVI) An Introduction and User's Guide," NASA TM 109147, November 1994.

18. Johnson, W., "A Comprehensive Analytical Model of Rotorcraft Aerodynamics and Dynamics," NASA TM 81182, June 1980.

19. Gallman, J. M., Tung, C., Schultz, K.-J., Splettstoesser, W., Buchholz, H., Spiegel, P., Burley, C. L., Brooks, T. F., Boyd, D. D. Jr., "Effect of Wake Structure on Blade-Vortex Interaction Phenomena: Acoustic Prediction and Validation," 16th AIAA Aeroacoustic Conference, Munich, Germany, June 1995.

20. Hassan, A. A., Charles, B. D., Tadghighi, H., Burley, C. L., "A Consistent Approach For Modeling The Aerodynamics of Self-Generated Rotor Blade-Vortex Interactions," 49th AHS Annual Forum, St. Louis., MO, May 1993.

21. Lau, B. H., Wadcock, A., Heineck, J. T., "Wake Visualization of a Full-Scale Tilt Rotor in Hover," AHS Technical Specialists' Meeting for Rotorcraft Acoustics and Aerodynamics, Williamsburg, VA, October 1997.

22. Coyne, A. J., Bhagwat M. J., Leishman, J. G., "Investigation into the Rollup and Diffusion of Rotor Tip Vortices Using Laser Doppler Velocimetry," 53rd AHS Annual Forum, Washington, Virginia Beach, VA, May 1997.

23. Swanson, A. A., "Shadowgraph Flow Visualization of Isolated Tiltrotor and Rotor/Wing Wakes," 48th AHS Annual Forum, Washington, D.C., June 1992.

24. Meakin, R. L., "Unsteady Simulation of the Viscous Flow About a V-22 Rotor and Wing in Hover," AIAA Atmospheric Flight Mechanics Conference, Baltimore, MD, August 1995.

25. Fejtek, I. Roberts, L., "Navier-Stokes Computation of Wing/Rotor Interaction for a Tilt Rotor in Hover," AIAA Paper 91-070, 29th Aerospace Sciences Meeting, Reno, NV January 1991.

26. Hu, H., "A Tilt Rotor Tip-Shape Analysis Using CFD", AHS Technical Specialists' Meeting for Rotorcraft Acoustics and Aerodynamics, Williamsburg, VA, October 1997.

27. Young, L. A., Booth, E. R., Yamauchi, G. K., Botha, G., Dawson, S., "Overview of the Testing of a Small-Scale Proprotor" 55th AHS Annual Forum, Montreal, Canada, May 1999.

28. Booth, E. R., McCluer, M., Tadghighi, H., "Acoustic Characteristics of an Isolated Tiltrotor Model in the DNW," 55th AHS Annual Forum, Montreal, Canada, May 1999.

29. Swanson, S. McCluer, M., Swanson, A., Yamauchi, G. K., "Airloads Measurements from a 1/4-Scale V-22 Tilt Rotor Wind Tunnel Test," 25th European Rotorcraft Forum, Rome, Italy, September 1999.

30. Yamauchi, G. K., Burley, C. L., Mercker, E., Pengel, K., JanakiRam, R., "Flow Measurements of an Isolated Model Tiltrotor," 55th AHS Annual Forum, Montreal, Canada, May 1999.

31. Tadghighi, H., Rajagopalan, G., Burley, C. L., "Simulation of Tiltrotor Fountain Flow Field Effects Using a Finite Volume Technique – An Aero/Acoustic Study," 51st AHS Annual Forum, Fort Worth, Texas, May, 1995.

32. Tadghighi, H., "TIN2 Model Development & Enhancements – A Turbulence Ingestion Noise Prediction for Tiltrotor With Fountain Flow Effects," 55th AHS Annual Forum, Montreal, Canada, May 1999.

33. Bridgeman, J. O., Prichard, D. S., Caradonna, F. X., "The Development of a CFD Potential Method For the Analysis of Tilt-Rotors," AHS and Royal Aeronautical Society, Technical Specialists' Meeting on Rotorcraft Acoustics/Fluid Dynamics, Philadelphia, PA, Oct. 1991.

34. Bagai, A., and Leishman, J.G., "Rotor Free-Wake Modeling Using a Relaxation Technique-Including Comparison With Experimental Data," Journal of the American Helicopter Society, Vol. 20, No. 3, July 1995.

35. Charles, B. D., Hassan, A. A., "Airframe Interference Effects on Rotorcraft BVI," 55th AHS Annual Forum, Montreal, Canada, May 1999.

36. Lyrintzis, A. S., Koutsavdis, E. K., Berezin, C. R., Visintainer, J. A., Pollack, M. J., " An Evaluation of a Rotating Kirchhoff Acoustic Methodology," Journal of American Helicopter Society, Vol. 43, No. 1, Jan. 1998.

37. Berezin, C., Pollack, M., Visintainer, J, Lyrintzis, A., Koutsavdis, E., "Development and Practical Application of the Rotating Kirchhoff Method For the Prediction of HSI and BVI Noise," AHS Technical Specialists' Meeting for Rotorcraft Acoustics and Aerodynamics, Williamsburg, VA, October 1997.

38. Brentner, K. S., Lyrintzis, A. S., and Koutsavdis, E. K., "A Comparison of Computational Aeroacoustic Prediction Methods for Transonic Rotor Noise," 52nd AHS Annual Forum, Washington, D.C., June 1996.

39. Brentner, K. S. and Holland, P. C., "An Efficient and Robust Method for Computing Quadrupole Noise," American Helicopter Society Aeromechanics Specialist Conference, Fairfield County, CT, October 1995.

40. Brooks, T. F., Pope, D. S., Marcolini, M. A., "Airfoil Self-Noise and Prediction," NASA RP 1218, July 1989.

41. Burley, C. L., Brooks, T. F., Splettstoesser, W. R., Schultz, K.-J., Kube, R., Bucholtz, H., Wagner, W., Weitemeyer, W., "Blade Wake Interaction Noise For a Bo-105 Model Main Rotor," AHS Technical Specialists' Meeting for Rotorcraft Acoustics and Aerodynamics, Williamsburg, VA, October 1997.

42. Lucas, M. J., Marcolini, M. A., "Rotorcraft Noise Model," AHS Technical Specialists' Meeting for Rotorcraft Acoustics and Aerodynamics, Williamsburg, VA, October 1997.

43.Tadghighi, H., "An Aero/Acoustic Optimization Model – A Multi-Objective, Multi-Level Decomposition Based Optimization," 54th AHS Annual Forum, Washington, D.C., May 1998.

44. Beddoes, T. S., "Two and Three Dimensional Indicial Methods for Rotor Dynamic Airloads," AHS Specialists Meeting on Rotorcraft Dynamics, Arlington, TX, November 1998.

45. Beddoes, T. S., "A Near Wake Dynamic Model," AHS Specialists Meeting on Aerodynamics and Aeroacoustics, Arlington, Va, February, 1987.

46. Brentner, K.S., "Prediction of Helicopter Rotor Discrete Frequency Noise," NASA TM 87721, October 1986.

47. Brooks, T. F. and Burley. C. L., "A Wind Tunnel Wall Correction Model for Helicopters in Open, Closed, and Partially Open Rectangular Test Sections," NASA TM (to be published) November 1999.

48. Langer, H., Peterson, R., and Maier, T., "An Experimental Evaluation of Wind Tunnel Wall Correction Methods for Helicopter Performance," 52nd AHS Annual Forum, Washington, D.C., June 1996.

49. Betz, A., "Vehalten von Wirbelsystemen," Z.f.a.M.M., Vol. 12, No. 3, June 1932, see also translation: "Behavior of Vortex Systems," NACA TM 713, June 1933.

50. Brooks, T.F., Jolly, J.R, Jr., and Marcolini, M.A. "Helicopter Main-Rotor Noise — Determination of Source Contributions using Scaled Model Data,", NASA TP 2825, August 1988.

51. Gessow, A., and Myers, G. C., Jr., Aerodynamics of the Helicopter. New York: Frederick Ungar Publishing Company, 1952.

52. Brooks, T. F., Booth, E. R., Jr, "The Effects of Higher Harmonic Control on Blade-Vortex Interaction Noise and Vibration," Journal of the American Helicopter Society, Vol. 38, No. 3, 1993.

53. Brooks, T. F., Booth, E. R., Jr., Boyd, D. D. Jr., Splettstoesser, W. R., Schultz, K. J., Kube, R., Niesl, G., Streby, O., "HHC Study in the DNW to Reduce BVI Noise – An Analysis," AHS/RaeS International Technical Specialists Meeting – Rotorcraft Acoustics and Fluid Dynamics, Philadelphia, PA, October 1991.